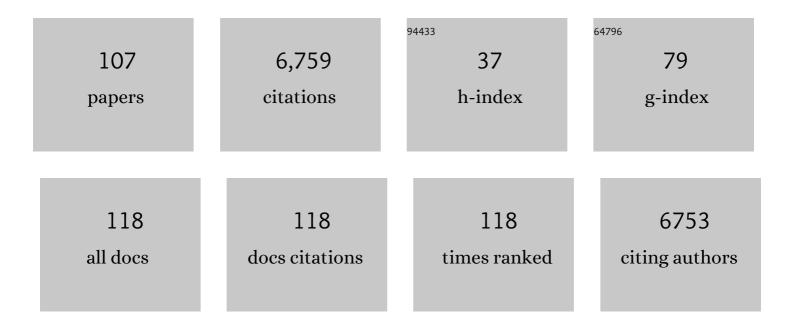
## **Patrick Scheerer**

List of Publications by Year in descending order

Source: https://exaly.com/author-pdf/13520/publications.pdf Version: 2024-02-01



#	Article	IF	CITATIONS
1	Crystal structure of opsin in its G-protein-interacting conformation. Nature, 2008, 455, 497-502.	27.8	1,019
2	Crystal structure of the ligand-free G-protein-coupled receptor opsin. Nature, 2008, 454, 183-187.	27.8	870
3	Crystal structure of metarhodopsin II. Nature, 2011, 471, 651-655.	27.8	620
4	The crystal structure of an oxygen-tolerant hydrogenase uncovers a novel iron-sulphur centre. Nature, 2011, 479, 249-252.	27.8	342
5	A G protein-coupled receptor at work: the rhodopsin model. Trends in Biochemical Sciences, 2009, 34, 540-552.	7.5	328
6	MC4R agonism promotes durable weight loss in patients with leptin receptor deficiency. Nature Medicine, 2018, 24, 551-555.	30.7	219
7	Structural Snapshots of Actively Translating Human Ribosomes. Cell, 2015, 161, 845-857.	28.9	161
8	Crystal structure of pre-activated arrestin p44. Nature, 2013, 497, 142-146.	27.8	156
9	Crystal structure of a common GPCR-binding interface for G protein and arrestin. Nature Communications, 2014, 5, 4801.	12.8	149
10	Structural Basis for Catalytic Activity and Enzyme Polymerization of Phospholipid Hydroperoxide Glutathione Peroxidase-4 (GPx4) <sup>,</sup> . <sup>,</sup> . Biochemistry, 2007, 46, 9041-9049.	2.5	138
11	Highly Conserved Residues Asp-197 and His-250 in Agp1 Phytochrome Control the Proton Affinity of the Chromophore and Pfr Formation. Journal of Biological Chemistry, 2007, 282, 2116-2123.	3.4	106
12	Position of Transmembrane Helix 6 Determines Receptor G Protein Coupling Specificity. Journal of the American Chemical Society, 2014, 136, 11244-11247.	13.7	105
13	A Ligand Channel through the G Protein Coupled Receptor Opsin. PLoS ONE, 2009, 4, e4382.	2.5	102
14	Double-flow focused liquid injector for efficient serial femtosecond crystallography. Scientific Reports, 2017, 7, 44628.	3.3	90
15	Crystal structure of a prokaryotic (6-4) photolyase with an Fe-S cluster and a 6,7-dimethyl-8-ribityllumazine antenna chromophore. Proceedings of the National Academy of Sciences of the United States of America, 2013, 110, 7217-7222.	7.1	89
16	Reversible [4Fe-3S] cluster morphing in an O2-tolerant [NiFe] hydrogenase. Nature Chemical Biology, 2014, 10, 378-385.	8.0	85
17	Molecular architecture of the ribosomeâ€bound Hepatitis C Virus internal ribosomal entry site <scp>RNA</scp> . EMBO Journal, 2015, 34, 3042-3058.	7.8	80
18	The complex of tmRNA–SmpB and EF-G on translocating ribosomes. Nature, 2012, 485, 526-529.	27.8	76

#	Article	IF	CITATIONS
19	A protonation-coupled feedback mechanism controls the signalling process in bathy phytochromes. Nature Chemistry, 2015, 7, 423-430.	13.6	74
20	Structural–Functional Features of the Thyrotropin Receptor: A Class A G-Protein-Coupled Receptor at Work. Frontiers in Endocrinology, 2017, 8, 86.	3.5	73
21	Effect of channel mutations on the uptake and release of the retinal ligand in opsin. Proceedings of the National Academy of Sciences of the United States of America, 2012, 109, 5247-5252.	7.1	71
22	Human endogenous retrovirus HERV-K(HML-2) RNA causes neurodegeneration through Toll-like receptors. JCI Insight, 2020, 5, .	5.0	68
23	Chromophore Structure of Cyanobacterial Phytochrome Cph1 in the Pr State: Reconciling Structural and Spectroscopic Data by QM/MM Calculations. Biophysical Journal, 2009, 96, 4153-4163.	0.5	66
24	Chromophore Heterogeneity and Photoconversion in Phytochrome Crystals and Solution Studied by Resonance Raman Spectroscopy. Angewandte Chemie - International Edition, 2008, 47, 4753-4755.	13.8	64
25	Structural snapshot of a bacterial phytochrome in its functional intermediate state. Nature Communications, 2018, 9, 4912.	12.8	62
26	Structural Basis for Two-component System Inhibition and Pilus Sensing by the Auxiliary CpxP Protein. Journal of Biological Chemistry, 2011, 286, 9805-9814.	3.4	59
27	Structures of ribosome-bound initiation factor 2 reveal the mechanism of subunit association. Science Advances, 2016, 2, e1501502.	10.3	59
28	Recurrent convergent evolution at amino acid residue 261 in fish rhodopsin. Proceedings of the National Academy of Sciences of the United States of America, 2019, 116, 18473-18478.	7.1	59
29	Structure of the Biliverdin Cofactor in the Pfr State of Bathy and Prototypical Phytochromes. Journal of Biological Chemistry, 2013, 288, 16800-16814.	3.4	58
30	Structural mechanism of arrestin activation. Current Opinion in Structural Biology, 2017, 45, 160-169.	5.7	55
31	Assembly of Synthetic Locked Chromophores with Agrobacterium Phytochromes Agp1 and Agp2. Journal of Biological Chemistry, 2006, 281, 28162-28173.	3.4	50
32	Structural and kinetic modeling of an activating helix switch in the rhodopsin-transducin interface. Proceedings of the National Academy of Sciences of the United States of America, 2009, 106, 10660-10665.	7.1	47
33	The Class III Cyclobutane Pyrimidine Dimer Photolyase Structure Reveals a New Antenna Chromophore Binding Site and Alternative Photoreduction Pathways. Journal of Biological Chemistry, 2015, 290, 11504-11514.	3.4	46
34	Structural and functional basis of phospholipid oxygenase activity of bacterial lipoxygenase from Pseudomonas aeruginosa. Biochimica Et Biophysica Acta - Molecular and Cell Biology of Lipids, 2016, 1861, 1681-1692.	2.4	46
35	Crystal structure and functional characterization of selenocysteine-containing glutathione peroxidase 4 suggests an alternative mechanism of peroxide reduction. Biochimica Et Biophysica Acta - Molecular and Cell Biology of Lipids, 2018, 1863, 1095-1107.	2.4	45
36	Krypton Derivatization of an O <sub>2</sub> â€Tolerant Membraneâ€Bound [NiFe] Hydrogenase Reveals a Hydrophobic Tunnel Network for Gas Transport. Angewandte Chemie - International Edition, 2016, 55, 5586-5590.	13.8	42

#	Article	IF	CITATIONS
37	The Crystal Structures of the N-terminal Photosensory Core Module of Agrobacterium Phytochrome Agp1 as Parallel and Anti-parallel Dimers. Journal of Biological Chemistry, 2016, 291, 20674-20691.	3.4	41
38	Tracking the route of molecular oxygen in O <sub>2</sub> -tolerant membrane-bound [NiFe] hydrogenase. Proceedings of the National Academy of Sciences of the United States of America, 2018, 115, E2229-E2237.	7.1	41
39	Structures of active melanocortin-4 receptor–Gs-protein complexes with NDP-α-MSH and setmelanotide. Cell Research, 2021, 31, 1176-1189.	12.0	40
40	Lightâ€Induced Conformational Changes of the Chromophore and the Protein in Phytochromes: Bacterial Phytochromes as Model Systems. ChemPhysChem, 2010, 11, 1090-1105.	2.1	39
41	Key Amino Acids in the Bacterial (6-4) Photolyase PhrB from Agrobacterium fabrum. PLoS ONE, 2015, 10, e0140955.	2.5	32
42	Lightâ€Induced Activation of Bacterial Phytochrome Agp1 Monitored by Static and Timeâ€Resolved FTIR Spectroscopy. ChemPhysChem, 2010, 11, 1207-1214.	2.1	31
43	Conserved Tyr223 <sup>5.58</sup> Plays Different Roles in the Activation and G-Protein Interaction of Rhodopsin. Journal of the American Chemical Society, 2011, 133, 7159-7165.	13.7	30
44	Resonance Raman Spectroscopic Analysis of the [NiFe] Active Site and the Proximal [4Fe-3S] Cluster of an O <sub>2</sub> -Tolerant Membrane-Bound Hydrogenase in the Crystalline State. Journal of Physical Chemistry B, 2015, 119, 13785-13796.	2.6	30
45	Crystallization and preliminary X-ray crystallographic analysis of the N-terminal photosensory module of phytochrome Agp1, a biliverdin-binding photoreceptor from Agrobacterium tumefaciens. Journal of Structural Biology, 2006, 153, 97-102.	2.8	29
46	The crystal structure of Pseudomonas aeruginosa lipoxygenase Ala420Gly mutant explains the improved oxygen affinity and the altered reaction specificity. Biochimica Et Biophysica Acta - Molecular and Cell Biology of Lipids, 2017, 1862, 463-473.	2.4	26
47	The Axonal Membrane Protein PRG2 Inhibits PTEN and Directs Growth to Branches. Cell Reports, 2019, 29, 2028-2040.e8.	6.4	25
48	Signal Transduction and Pathogenic Modifications at the Melanocortin-4 Receptor: A Structural Perspective. Frontiers in Endocrinology, 2019, 10, 515.	3.5	24
49	Design of a light-gated proton channel based on the crystal structure of <i>Coccomyxa</i> rhodopsin. Science Signaling, 2019, 12, .	3.6	24
50	Differential Signaling Profiles of MC4R Mutations with Three Different Ligands. International Journal of Molecular Sciences, 2020, 21, 1224.	4.1	24
51	Phytochromes from <i>Agrobacterium fabrum</i> . Photochemistry and Photobiology, 2017, 93, 642-655.	2.5	23
52	The Trace Amine-Associated Receptor 1 Agonist 3-lodothyronamine Induces Biased Signaling at the Serotonin 1b Receptor. Frontiers in Pharmacology, 2018, 9, 222.	3.5	22
53	The structure of the antiâ€câ€myc antibody 9E10 Fab fragment/epitope peptide complex reveals a novel binding mode dominated by the heavy chain hypervariable loops. Proteins: Structure, Function and Bioinformatics, 2008, 73, 552-565.	2.6	21
54	Common Structural Elements in the Chromophore Binding Pocket of the Pfr State of Bathy Phytochromes. Photochemistry and Photobiology, 2017, 93, 724-732.	2.5	21

#	Article	IF	CITATIONS
55	Tight association of N-terminal and catalytic subunits of rabbit 12/15-lipoxygenase is important for protein stability and catalytic activity. Biochimica Et Biophysica Acta - Molecular and Cell Biology of Lipids, 2011, 1811, 1001-1010.	2.4	19
56	Structure-Based Biophysical Analysis of the Interaction of Rhodopsin with G Protein and Arrestin. Methods in Enzymology, 2015, 556, 563-608.	1.0	19
57	Melanocortin Receptor Accessory Protein 2-Induced Adrenocorticotropic Hormone Response of Human Melanocortin 4 Receptor. Journal of the Endocrine Society, 2019, 3, 314-323.	0.2	19
58	MicroRNA-100-5p and microRNA-298-5p released from apoptotic cortical neurons are endogenous Toll-like receptor 7/8 ligands that contribute to neurodegeneration. Molecular Neurodegeneration, 2021, 16, 80.	10.8	18
59	Insights into Basal Signaling Regulation, Oligomerization, and Structural Organization of the Human G-Protein Coupled Receptor 83. PLoS ONE, 2016, 11, e0168260.	2.5	16
60	Dynein light chain 8a of <i>Toxoplasma gondii</i> , a unique conoidâ€localized βâ€strandâ€swapped homodimer, is required for an efficient parasite growth. FASEB Journal, 2013, 27, 1034-1047.	0.5	15
61	The intramolecular agonist is obligate for activation of glycoprotein hormone receptors. FASEB Journal, 2020, 34, 11243-11256.	0.5	15
62	Insights into functional aspects of centrins from the structure of N-terminally extended mouse centrin 1. Vision Research, 2006, 46, 4568-4574.	1.4	14
63	The Activation Pathway of Human Rhodopsin in Comparison to Bovine Rhodopsin. Journal of Biological Chemistry, 2015, 290, 20117-20127.	3.4	14
64	A New Multisystem Disorder Caused by the Gαs Mutation p.F376V. Journal of Clinical Endocrinology and Metabolism, 2019, 104, 1079-1089.	3.6	14
65	Intramolecular Proton Transfer Controls Protein Structural Changes in Phytochrome. Biochemistry, 2020, 59, 1023-1037.	2.5	14
66	Intersubunit distances in full-length, dimeric, bacterial phytochrome Agp1, as measured by pulsed electron-electron double resonance (PELDOR) between different spin label positions, remain unchanged upon photoconversion. Journal of Biological Chemistry, 2017, 292, 7598-7606.	3.4	13
67	Mechanistic insights into the role of prenyl-binding protein PrBP/δ in membrane dissociation of phosphodiesterase 6. Nature Communications, 2018, 9, 90.	12.8	13
68	An incretin-based tri-agonist promotes superior insulin secretion from murine pancreatic islets via PLC activation. Cellular Signalling, 2018, 51, 13-22.	3.6	13
69	Role of the Propionic Side Chains for the Photoconversion of Bacterial Phytochromes. Biochemistry, 2019, 58, 3504-3519.	2.5	13
70	Role of Structural Dynamics at the Receptor G Protein Interface for Signal Transduction. PLoS ONE, 2015, 10, e0143399.	2.5	12
71	Crystal Structures of Bacterial (6â€4) Photolyase Mutants with Impaired DNA Repair Activity. Photochemistry and Photobiology, 2017, 93, 304-314.	2.5	12
72	Structural Complexity and Plasticity of Signaling Regulation at the Melanocortin-4 Receptor. International Journal of Molecular Sciences, 2020, 21, 5728.	4.1	12

#	Article	IF	CITATIONS
73	Ultrafast proton-coupled isomerization in the phototransformation of phytochrome. Nature Chemistry, 2022, 14, 823-830.	13.6	12
74	The Lumi-R Intermediates of Prototypical Phytochromes. Journal of Physical Chemistry B, 2020, 124, 4044-4055.	2.6	10
75	Local Electric Field Changes during the Photoconversion of the Bathy Phytochrome Agp2. Biochemistry, 2021, 60, 2967-2977.	2.5	10
76	The arrestin-1 finger loop interacts with two distinct conformations of active rhodopsin. Journal of Biological Chemistry, 2018, 293, 4403-4410.	3.4	9
77	Binding, Thermodynamics, and Selectivity of a Non-peptide Antagonist to the Melanocortin-4 Receptor. Frontiers in Pharmacology, 2018, 9, 560.	3.5	9
78	Divalent Cations Increase DNA Repair Activities of Bacterial (6â€4) Photolyases. Photochemistry and Photobiology, 2017, 93, 323-330.	2.5	8
79	Light- and temperature-dependent dynamics of chromophore and protein structural changes in bathy phytochrome Agp2. Physical Chemistry Chemical Physics, 2021, 23, 18197-18205.	2.8	8
80	On the Role of the Conserved Histidine at the Chromophore Isomerization Site in Phytochromes. Journal of Physical Chemistry B, 2021, 125, 13696-13709.	2.6	8
81	Autoantibodies Targeting AT1- and ETA-Receptors Link Endothelial Proliferation and Coagulation via Ets-1 Transcription Factor. International Journal of Molecular Sciences, 2022, 23, 244.	4.1	8
82	A coleopteran triosephosphate isomerase: Xâ€ray structure and phylogenetic impact of insect sequences. Insect Molecular Biology, 2010, 19, 35-48.	2.0	7
83	Phytochromes in Agrobacterium fabrum. Frontiers in Plant Science, 2021, 12, 642801.	3.6	7
84	Angiotensin and Endothelin Receptor Structures With Implications for Signaling Regulation and Pharmacological Targeting. Frontiers in Endocrinology, 2022, 13, 880002.	3.5	7
85	Structure of an antiâ€cholera toxin antibody Fab in complex with an epitopeâ€derived <scp>D</scp> â€peptide: a case of polyspecific recognition. Journal of Molecular Recognition, 2007, 20, 263-274.	2.1	6
86	Crystallization and preliminary X-ray crystallographic analysis of the [NiFe]-hydrogenase maturation factor HypF1 from <i>Ralstonia eutropha</i> H16. Acta Crystallographica Section F: Structural Biology Communications, 2010, 66, 452-455.	0.7	6
87	Use of a sequential high throughput screening assay to identify novel inhibitors of the eukaryotic SRP-Sec61 targeting/translocation pathway. PLoS ONE, 2018, 13, e0208641.	2.5	6
88	Photoinduced reaction mechanisms in prototypical and bathy phytochromes. Physical Chemistry Chemical Physics, 2022, 24, 11967-11978.	2.8	6
89	Crystallization and preliminary X-ray studies of mouse centrin1. Acta Crystallographica Section F: Structural Biology Communications, 2005, 61, 510-513.	0.7	5
90	Functional differences between TSHR alleles associate with variation in spawning season in Atlantic herring. Communications Biology, 2021, 4, 795.	4.4	5

#	Article	IF	CITATIONS
91	Molecular Effects of Auto-Antibodies on Angiotensin II Type 1 Receptor Signaling and Cell Proliferation. International Journal of Molecular Sciences, 2022, 23, 3984.	4.1	5
92	Molecular basis for the catalytic inactivity of a naturally occurring near-null variant of human ALOX15. Biochimica Et Biophysica Acta - Molecular and Cell Biology of Lipids, 2013, 1831, 1702-1713.	2.4	4
93	Ein Netzwerk aus hydrophoben Tunneln zum Transport gasförmiger Reaktanten in einer O <sub>2</sub> â€toleranten, membrangebundenen [NiFe]―Hydrogenase, aufgedeckt durch Derivatisierung mit Krypton. Angewandte Chemie, 2016, 128, 5676-5680.	2.0	4
94	The Pathogenic TSH β-subunit Variant C105Vfs114X Causes a Modified Signaling Profile at TSHR. International Journal of Molecular Sciences, 2019, 20, 5564.	4.1	4
95	Phytochrome Mediated Responses in Agrobacterium fabrum: Growth, Motility and Plant Infection. Current Microbiology, 2021, 78, 2708-2719.	2.2	4
96	Resonance Raman spectroscopic analysis of the iron–sulfur cluster redox chain of the Ralstonia eutropha membraneâ€bound [NiFe]â€hydrogenase. Journal of Raman Spectroscopy, 0, , .	2.5	4
97	Zebrafish Bioassay for Screening Therapeutic Candidates Based on Melanotrophic Activity. International Journal of Molecular Sciences, 2021, 22, 9313.	4.1	2
98	Crystallization and Preliminary X-ray Analysis of Complexes of Porcine Pancreatic Elastase with two Natural Inhibitors. Protein and Peptide Letters, 2004, 11, 393-399.	0.9	2
99	Expression and Characterization of Relaxin Family Peptide Receptor 1 Variants. Frontiers in Pharmacology, 2021, 12, 826112.	3.5	2
100	Evaluation of a rare glucoseâ€dependent insulinotropic polypeptide receptor variant in a patient with diabetes. Diabetes, Obesity and Metabolism, 2019, 21, 1168-1176.	4.4	1
101	Two photolyases in Agrobacterium tumefaciens. FASEB Journal, 2015, 29, 879.22.	0.5	1
102	A cytosolic disulfide bridgeâ€supported dimerization is crucial for stability and cellular distribution of Coxsackievirus B3 protein 3A. FEBS Journal, 2022, 289, 3826-3838.	4.7	1
103	Dynamics of C-Terminal Gtl $\pm$ and Gsl $\pm$ Peptides in the Binding Cavity of Active GPCRs. Biophysical Journal, 2013, 104, 538a.	0.5	0
104	Conformational Dynamics During GPCR - G Protein Coupling. Biophysical Journal, 2014, 106, 37a.	0.5	0
105	Protein structures guide the design of a much-needed tool for neuroscience. Nature, 2018, 561, 312-313.	27.8	0
106	Structures of the photosensory core module of bacteriophytochrome Agp1 from two crystal forms reveal plasticity of the Pr state. Acta Crystallographica Section A: Foundations and Advances, 2016, 72, s228-s229.	0.1	0
107	Methodical tools for the structural elucidation of G-protein coupled receptors. Endocrine Abstracts, 0, , .	0.0	0